The Influence Of Human Movement On Transport Of Airborne Infectious Particles In Hospital Premises

Jinliang Wang, Tin-Tai Chow *, Zhang Lin

Building Energy and Environmental Technology Research Unit, Division of Building Science and Technology, City University of Hong Kong, Tat Chee Avenue, Kowloon, Hong Kong SAR, China

ABSTRACT

In hospital premises, where the requirement of controlling cross infection is demanding, the impact of human movement on transport of airborne infectious particles (AIPs) is rarely investigated. In this study, the impacts of human movement on distribution of AIPs in two highly infectious hospital environments, i.e. airborne infection isolation room (AIIR) and operating theatre (OT) are investigated numerically. In the case of AIIR, the influence of different walking speeds on the distribution of respiratory droplets is investigated by adopting Lagrangian method for tracing the motion of droplets, dynamic mesh model for describing human walking, and Eulerian RANS model for solving airflow. In the case of OT, the impact of surgeon bending movement on distribution of bacteria-carrying particles (BCPs) is dynamically simulated by applying the similar numerical method as in the AIIR case, except that the drift-flux model is used for modelling BCPs distribution. The adopted models are first successfully validated against literature data. The results show that, in the case of AIIR walking speed could effectively change the overall numbers of suspended droplets and faster walking speed is more favorable to reduce the overall numbers of suspended droplets. In the case of OT, 45^{o} bending posture for performing operation and bending back movement of the surgeon can cause the concentration of BCPs within the surgical critical zone exceeding the recommended 10 cfu/m^3, while for the 2-second bending over process as well as the 30-second standing upright posture for rest the concentration of BCPs within the surgical critical zone can be generally less than 10 cfu/m^3. Therefore, lack of considering the influence of human movement in hospital premises may ignore some important phenomena related to nosocomial infection and consequently misinterpret the nosocomial infection risk. More in-depth studies in this area should be done in the future.

KEYWORDS

Airborne infectious particles, Human movement, AII room, Operating theatre, Computational fluid dynamics

* Corresponding author email: bsttchow@cityu.edu.hk

INTRODUCTION

Recent research works have shown that human movement can lead to very strong secondary airflow and consequently influence the distribution of airborne infectious particles (AIPs). Examples in hospitals are the dispersion of bacteria-carrying particles (BCPs) in operating theatre (OT) and respiratory droplets exhaled by patients with infectious diseases. Brohus et al. (2006) found that the movement of scrub nurse can cause the bacteria transport from less clean zone to the ultraclean zone in OT. Tang et al. (2006) reported that the movement of people in a room plays a significant role in disturbing the airflow and also in transporting infected air from one place to another. The experimental work of Bjørn and Nielsen (2002) found that a moving person could create quite strong air movement and destroy the boundary layer around human body. Mazumdar et al. (2010) numerically investigated the effects of different human activities on the contaminant concentration distribution in a single inpatient ward. However, all these related works just simply substituted gas contaminant for AIPs. Actually, the transport characteristics of particles can be quite different from those of gaseous counterparts due to gravitational settlement and inertia effect etc. Directly using gaseous surrogate instead of AIPs to carry out related research may not truly reflect the real situations. In highly infectious hospital premises like operating theatre (OT) and airborne infection isolation room (AIIR), the requirement of controlling cross infection of diseases is very demanding. However, the investigations on the influence of human movement on AIPs distribution are so far inadequate, most probably due to the complexity of considering human movement. In this study, the impacts of human movement on the distribution of AIPs in AIIR and OT are respectively investigated.

AIIR CASE

A. Physical model of AIIR

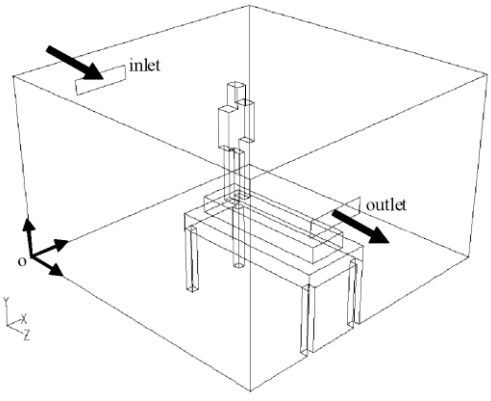

Figure 1. *Physical model of AIIR*

Our physical model of AIIR, 4.0m (x) × 2.5m (y) × 4.0m (z), is similar to the one adopted by Shih et al. (2007) shown in Figure 1, except that our lying patient is represented by a block of 1.73m (height) ×0.2m (thickness) ×0.5m (width). In this case, the size of the patient mouth when coughing is 0.01 ×0.02 m^2. The coughing initial velocity of droplets is taken as 22m/s, with four droplet sizes of 0.5μm, 5μm, 10μm and 20μm. The overall numbers of droplets

coughed out are 10000, with equal allocation to each size. The density of droplets is 600kg/m^3. The walking man is initially positioned at 0.75m away from the wall with the supply inlet. His straight-line walking along z direction is assumed to be back and forth for one time, during which the overall walking distance is 5.0m. He will remain stationary afterwards. Three steady walking speeds of 0.25m/s, 0.5m/s and 1.0m/s are respectively investigated in this study.

B. Mathematical model

In this AIIR airflow study, the RANS (Reynolds averaged Navier-Stokes) method with standard $k-\varepsilon$ turbulence model considering buoyancy effect is used, which is similar to the work of Shih et al. (2007). The governing equations, including continuity, momentum, energy, turbulent kinetic energy k and turbulent dissipation rate ε, can be written in the following format:

$$\frac{\partial(\rho\phi)}{\partial t}+\nabla\cdot(\rho\phi\vec{V})=\nabla\cdot(\Gamma_\phi\nabla\phi)+S_\phi \tag{1}$$

where ρ is the air density; $\vec{V}$ is the velocity vector; ϕ represents each of the three velocity components u, v, w, turbulent kinetic energy k, turbulent dissipation rate ε and air enthalpy H; Γ_ϕ is the effective diffusion coefficient for each dependent variable; and S_ϕ is the source term. When $\phi=1$, the equation becomes the continuity equation. More details about this model can be found in Shih et al. (2007). The QUICK scheme is adopted for the discretization of the equations and the SIMPLEC algorithm is used to couple pressure and velocity. The standard wall function is employed to treat the turbulent flow properties in the near wall regions. The boundary conditions in this study are kept the same as those in Shih et al. (2007).

For tracking the movement of droplets coughed out, the Lagrangian method is applied. According to Chen and Zhao (2010), the evaporation effect of droplets with sizes concerned in this study can be neglected. Herein the droplets are treated as droplet nuclei for simulation. For a particle, the force balance in the i-direction can be written as:

$$\frac{du_{pi}}{dt}=\frac{(u_i-u_{pi})}{\tau}+\frac{g_i\cdot(\rho_p-\rho)}{\rho_p}+F_{ai} \tag{2}$$

where u_i and u_{pi} are respectively the velocity of air and particles (m/s); g_i is the gravitational acceleration (m/s^2); τ is the particle relaxation time; ρ_p and ρ are the density of particle and air respectively (kg/m^3); and F_{ai} considers the Brownian force, Saffman's lift force and thermophoretic force. In addition, the effect of turbulent dispersion on particles is considered by the discrete random walk (DRW) model.

Regarding the simulation of walking human, the dynamic mesh model is adopted with the general form as follows:

$$\frac{d}{dt}\int_V \rho\phi dV + \int_{\partial V} \rho\phi(\vec{u}-\vec{u}_g)\cdot d\vec{A} = \int_{\partial V} \Gamma\nabla\phi\cdot d\vec{A} + \int_V S_\phi dV \quad (3)$$

where $\vec{u}$ is the flow velocity vector; $\vec{u}_g$ is the grid velocity of the moving mesh; Γ is the diffusion coefficient, and ∂V represents the boundary of the control volume. The dynamic layering method is used to add or move layers of cells adjacent to moving boundaries. To avoid large-scale mesh update, the whole mesh domain is divided into "static" and "dynamic" zones. After a successful grid independence test, a grid with 531,907 cells is finally used for computation. The aforementioned mathematical model has been well validated against literature data, which can be found in our previous work (Wang and Chow 2011).

OT CASE

A. Details of OT studied

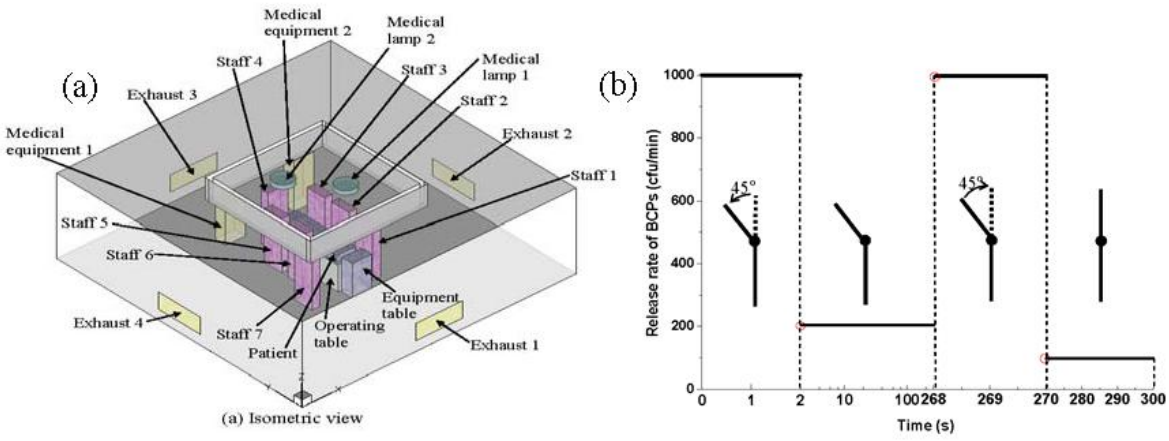

***Figure 2**. (a)Geometrical configuration of OT (b) Release rate of BCPs from staff 2 in a 5-minute bending cycle*

Figure 2(a) shows the square-shape standard OT, 7 m (length) × 7 m (width) × 2.7 m (height), in this case study. The same physical model was adopted in our previous research (Chow et al. 2006). The OT is served by a vertical-flow ultraclean ventilation (UCV) system in accordance with the HTM 03-01 (2007) recommendations. The perforated ceiling diffuser is 2.8 m × 2.8 m, with the partial walls terminated at 2.0 m above the floor level for strengthening the unidirectional flow. The air is exhausted through four 1.2 m × 0.55 m low-level outlets, which are located at the mid-plane of the four side walls. According to HTM 03-01 (2007), the average air velocity at 2 m above floor level should be at 0.38 m/s. This is able to provide a washing effect against the settlement of airborne BCPs shedding from surgical staff, such as skin scales. And it is expected that in the critical area within 300mm of the wound, the ultra-clean air with less than 10cfu/m^3 can be achieved. Hence in this study the air supply velocity is set as 0.38m/s with a supply temperature of 20℃. And to prevent the BCPs infection from outside of the OT the whole OT is kept under a positive pressure of 25 Pa.

More details about the equipments, the surgical team and their heat release conditions can be found in our previous article (Chow et al. 2006). To investigate the influence of surgeon bending movement on the BCPs distribution, two scenarios were simulated separately and then compared. The first scenario involves all surgical staff standing upright without movement. The second one considers a 30-minute periodic bending movement of surgical staff 2 with other motionless staff standing upright. One periodic cycle of the bending movement is taken as 5 minutes. The release rates of BCPs in one cycle are given in Figure 2(b). In this study BCPs with diameters of 5 μm, 6 μm, 8 μm and 10 μm are chosen as representative infectious particles.

B. Mathematical model

For simulating the airflow in OT with characteristics of relatively low turbulence and non-dominant buoyancy, the standard $k-\varepsilon$ turbulence model is used. The same was also applied in our previous work (Chow et al. 2006). The general form of the governing equations for continuity, momentum, energy, turbulent kinetic energy and turbulent dissipation rate is the same as Eq. (1). Since the overall cooling load in the OT is 2500 W, the thermal buoyancy effect is handled by the Boussinesq model, whereas the thermal radiation effect is by the discrete ordinates radiation model. For modeling particles transport indoors, a modified drift-flux model (MDFM) based on the Eulerian-Eulerian method is adopted due to its convenience for postprocessing particle concentration. The governing equation of particle concentration can be expressed as:

$$\frac{\partial C}{\partial t}+\nabla\cdot[(\vec{V}+\vec{v}_s)\cdot C]=\nabla\cdot[(D+\varepsilon_p)\cdot\nabla C]+S_c \qquad (4)$$

where C is the particle number concentration; $\vec{V}$ and $\vec{v}_s$ are respectively the velocity of air and gravitational settling of particle; D is the Brownian diffusivity of particle; ε_p is the particle turbulent diffusivity; and S_c is the particle source term. In the particle concentration core region S_c takes a value of zero, while in the near-wall concentration boundary layer S_c considers particles deposition losses. More details about MDFM can be referred to Zhao et al. (2004).

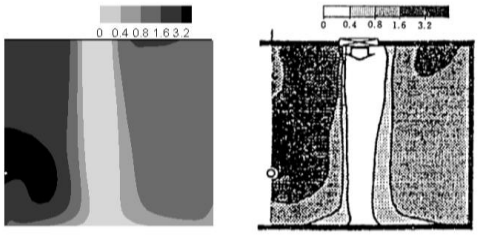

Figure 3*. Validation of present simulation against measurements of Murakami et al. (1992)*

To model the bending movement of surgeon 2, the dynamic mesh model with general Eq. (3) is again adopted. After the grid independence tests, tetrahedral cells that vary from 84,512 to 113,591 in total numbers are used for the dynamic mesh zone, and 234,976 hexahedral cells are generated for the static mesh zone. Since both the standard $k-\varepsilon$ turbulence model for airflow and the dynamic mesh model for human movement were successfully validated in our

previous works, in this study only the MDFM for describing BCPs transport needs to be validated. Herein, we fully followed the experiments of Murakami et al. (1992) to execute numerical simulation by applying the drift-flux model. From Figure 3 it can be seen that the dimensionless particle concentration comparison of our simulation results with the measurements of Murakami et al. (1992) can agree very well.

RESULTS

A. Influence of human walking on distribution of droplets

Figure 4(a) shows the velocity distribution at x=3 m at time=2.5s and walking speed of 1.0m/s. It can be seen that when the man walks towards the wall with the air outlet, there exist two recirculation zones: an upper zone close to the upper back of the human head and a lower zone around the lower part of the human back. Therefore, human walking can disturb local airflow significantly.

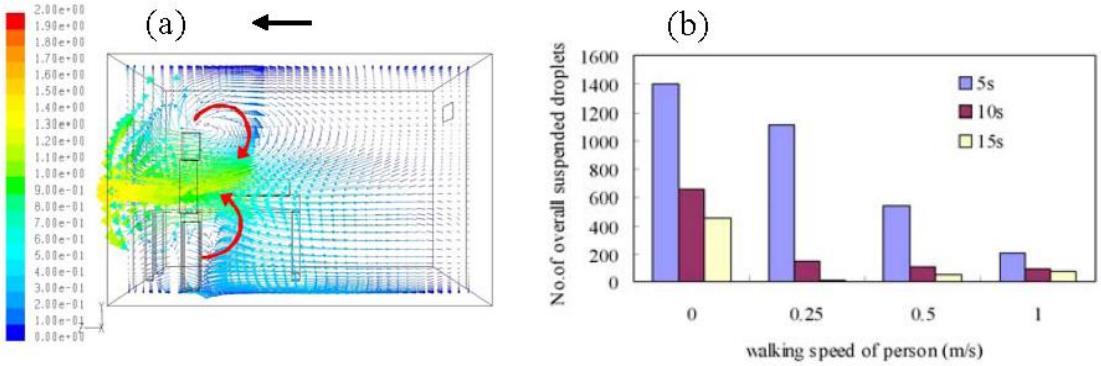

Figure 4*. (a)Velocity vector distribution at x=3m at time=2.5s and walking speed of 1.0m/s (b)Number of overall suspended droplets at different time instants and walking speeds*

Figure 4(b) shows the number of overall suspended droplets remained in room air at different time instants and walking speeds. It can be seen that the increase of walking speed can effectively reduce the amount of suspended droplets in the room. This is by accelerating the escaped amount via the air outlet. As a consequence, the infection risk is reduced. For instance, when the walking speed (of a healthcare worker) increases to 1m/s, within 5s the number of overall suspended droplets can decrease as much as 98%.

B. Influence of surgeon bending on BCPs distribution

For the first scenario without human movement, the steady concentration distribution of BCPs at z=1.1 is shown in Figure 5(a). It can be seen that the concentration of BCPs within the surgical critical zone can become less than 1 cfu/m^3 due to the downward washing effect, which complies with the recommended value of less than 10 cfu/m^3 from HTM 03-01 (2007).

The second scenario considers the sole bending movement of surgeon 2. The overall 30-minute minor surgery consists of 6 periodic cycles, of which one cycle is shown in Figure 2(b). During one bending movement cycle of 300 seconds, the movements can be subdivided into four sessions, viz, 2-second bending over process, 266-second 45^o bending posture for

performing operation, 2-second bending back process, and 30-second standing upright posture for short rest. For the entire simulation process, the periodic unsteady state for both airflow and concentration distribution of BCPs can be achieved from the second cycle to the sixth cycle. Therefore, only BCPs distributions in the second cycle of the surgeon bending movement are discussed herein. It is found that for the 2-second bending over process as well as the 30-second standing upright posture for rest the concentration of BCPs within the surgical critical zone can be generally less than 10 cfu/m^3. Figure 5(b) shows the typical concentration distribution of BCPs when the surgical staff 2 performs operation with 45^o bending posture. It is found that during this period the concentration of BCPs within the 300 mm of the wound exceeds 10 cfu/m^3. For the 2-second bending back process of the staff 2, the concentration of BCPs within the surgical critical zone increases with time. Due to page limitation, we only show the concentration distribution of BCPs at the end of the bending back process (see Figure 5(c)). It can be clearly seen that within the surgical critical zone the concentration of BCPs may reach 250 cfu/m^3, which largely exceeds the recommended 10 cfu/m^3.

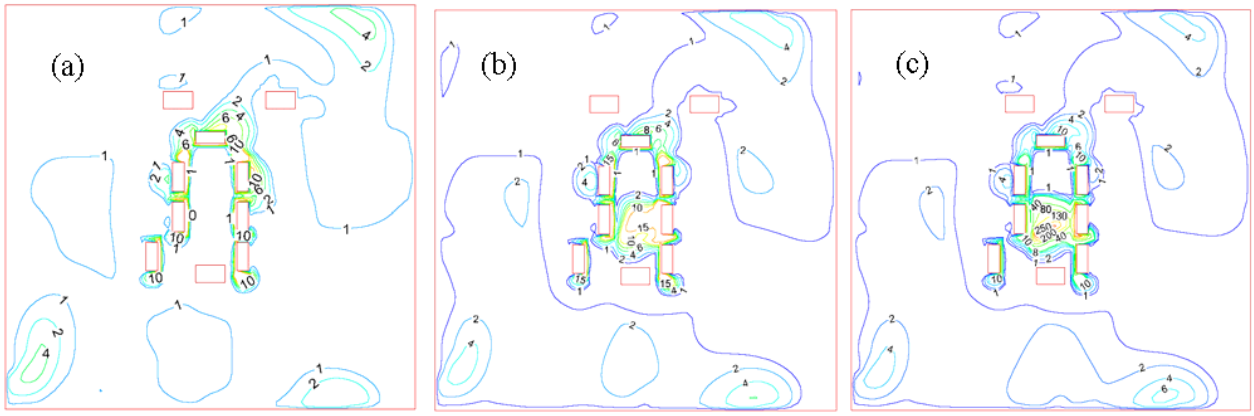

Figure 5*. Concentration of BCPs (unit: cfu/m^3) at z=1.1 (a) when all surgical staff standing upright without movement (b) when surgeon 2 performing operation with 45^o bending posture (c) at the end of bending back process*

DISCUSSION

From the above case studies, we can clearly see that the distribution of AIPs like respiratory droplets and BCPs in hospital premises can be largely influenced by human movement. Since the infection via AIPs can be acquired by short-term exposure of human, in hospital premises direct investigation on the influence of human movement on transport of AIPs is very essential. Lack of considering the influence of human movement in hospital premises may ignore some important aspects related to nosocomial infection and consequently misinterpret the nosocomial infection risk. In terms of numerical simulation, the particle resuspension and collision boundary condition between particles and moving human may influence the simulation accuracy, further efforts should be focused on those aspects. In addition, deliberate experimental study on the influence of human movement on transport of AIPs indoors should also be carried out.

CONCLUSIONS

In this study, the impacts of different human movements on the distribution of AIPs in AIIR and OT have been investigated via numerical analysis. The conclusions are summarized below:

(1) In the case of AIIR, human walking in AIIR can disturb local airflow significantly; faster walking speed could effectively reduce the overall numbers of suspended droplets.

(2) In the case of OT, 45^{o} bending posture for performing operation and bending back movement of the surgeon can cause the concentration of BCPs within the surgical critical zone exceeding the recommended 10 cfu/m^3, among which the 2-second bending back movement causes the highest BCPs concentration.

REFERENCES

Bjørn E and Nielsen PV. 2002. Dispersal of exhaled air and personal exposure in displacement ventilated rooms, *Indoor Air*. 12: 147 -164.

Brohus H, Balling KD and Jeppesen D. 2006. Influence of movements on contaminant transport in an operating room, *Indoor Air*. 16: 356-372.

Chen C and Zhao B. 2010. Some questions on dispersion of human exhaled droplets in ventilation room: answers from numerical investigation, *Indoor Air*. 20: 95–111.

Chow TT, Lin Z and Bai W. 2006. The integrated effect of medical lamp position and diffuser discharge velocity on ultra-clean ventilation performance in an operating theatre, *Indoor and Built Environment*. 15(4): 315-31.

Department of Health / Estates and Facilities Division 2007. *Health Technical Memorandum 03-01: Specialised ventilation for healthcare premises. Part A - Design and installation*. Quarry House, Quarry Hill, Leeds: Department of Health/Estates and Facilities Division.

Mazumdar S, Yin Y, Guity A, Marmion P, Gulick B and Chen Q. 2010. Impact of moving objects on contaminant concentration distributions in an inpatient room with displacement ventilation, *HVAC&R Research*. 16(5):545-64.

Murakami S, Kato S, Nagano S and Tanaka Y. 1992. Diffusion characteristics of airborne particles with gravitational settling in a convection-dominant indoor flow field, *ASHRAE Transactions*. 98 (Part 1): 82–97.

Shih YC, Chiu CC and Wang O. 2007. Dynamic airflow simulation within an isolation room, *Building and Environment*. 42:3194-209.

Tang JW, Li Y, Eames I, Chan PKS and Ridgway GL. 2006. Factors involved in the aerosol transmission of infection and control of ventilation in healthcare premises, *Journal of Hospital Infection*. 64: 100-14.

Wang JL and Chow TT. 2011. Numerical investigation of influence of human walking on dispersion and deposition of expiratory droplets in airborne infection isolation room, *Building and Environment*. 46: 1993-2002.

Zhao B, Li XT and Zhang Z. 2004. Numerical study of particle deposition in two differently ventilated rooms, *Indoor and Built Environment*. 13:443–451.